Improving Thermal Contact Conductance from Electronics Board to Rack Infrastructure

Jeroen Terpstra[1], Wessel W. Wits[1,2]*

[1] Thales Nederland B.V., Hengelo, Netherlands
[2] University of Twente, Enschede, Netherlands

* Corresponding Author: Wessel.Wits@nl.thalesgroup.com, +31 6 1842 3661

Abstract

This paper presents experimental results of thermal contact conductance between an electronics board and rack infrastructure. For line replaceable units using liquid conduction cooling, the baseplate-cold plate interface introduces a critical thermal resistance. Using a dedicated experimental set-up that measures temperature gradients across such interfaces, this study systematically analyses key design parameters, such as surface roughness, contact pressure, coatings, such as nickel and tin plating, and the application of indium as thermal interface material. Limitations of theoretical models are addressed demonstrating the importance of experimental testing. Empirical results of this study show that cold plate plating and the use of indium have the most impact on the interface heat transfer coefficient. The presented results enable design engineers to improve thermal contact conductance thereby extending the range of liquid conduction cooling for cases in which electronics boards are clamped into a rack infrastructure.

1   Background

Cooling of electronics equipment for high-end applications is becoming more stringent than ever [1]. Increasing power densities demand short and optimized heat flow paths. However, this generally negatively impacts the operational availability of these systems as the integration of electronic components often reduces its maintainability.

In the cooling methodology of Liquid Conduction Cooling (LCC) a trade-off is made regarding maintainability and cooling performance on the one hand and cost savings on the other hand [2]. This is accomplished by having a configuration in which conduction-cooled Line Replaceable Units (LRUs) are clamped in a liquid-cooled rack, as shown in Figure 1.
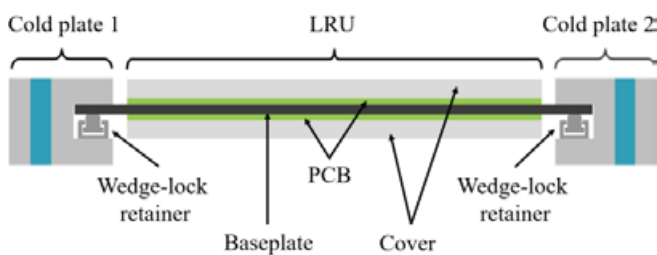

Figure 1: Liquid Conduction Cooling (LCC) configuration.

The LRU in this case has a conducting metal baseplate onto which Printed Circuit Boards (PCBs) and other electronic packages are mounted. The baseplate is inserted and clamped into the cold plate racks by means of wedge-lock retainers. Such retainers consist of multiple wedge-shaped sliding elements that are pushed together by tightening a screw to exert a force, as shown in Figure 2.

Figure 2: Working principle of a wedge-lock retainer.

Regarding the heat flow path, a critical thermal resistance for LCC is the baseplate-cold plate (i.e. board to rack) interface. This resistance is directly coupled to the performance of the wedge-lock retainer that has a number of drawbacks regarding its performance. Firstly, internal friction of the sliding segments causes an unpredictable level of specific pressure. Secondly, the exerted pressure is non-uniformly distributed being merely concentrated at the locations where the segments contact each other.

This is demonstrated in Figure 3, in which the retainer was claimed onto a pressure sensitive foil. Darker markings on the foil, indicating the highest pressure, are typically located near connecting segments. Presumably, during tightening also a bending moment is introduced. Altogether, this makes the retainer an interesting topic for optimization what is also eminent from the relatively large number of patents for alternative designs [3-7].

Figure 3: Pressure distribution of a wedge-lock retainer visualized by a pressure sensitive foil.

The cooling path between the electronics board and rack infrastructure is conduction based. Modelling the heat flow through solid materials can be done reasonably accurate. Modelling the interface between the board and rack is however dependent on design, manufacturing and assembly parameters. As the board and rack are clamped, typical optimization strategies are reducing surface roughness, increasing the clamping force, introducing an interstitial medium, such as a Thermal Interface Material (TIM), etc.

Optimizing LCC up to the last degree is essential, as redesigning the cooling infrastructure using news coolign principles, such as phase-change principles, is a massive undertaking. Therefore, the aim of this study is to understand the influence of relevant design, manufacturing and assembly parameters of the electronics board to rack infrastructure. For this, a theoretical model is constructed and an experimental set-up was built to validate model findings through a design of experiments. Finally, the Thermal Contact Conductance (TCC) was optimized for the application at hand, including aspects as cost, ease of assembly, reliability, ease of maintenance, etc.

2   Thermal contact conductance modelling

A theoretical model describing TCC has been developed by Yovanovich and Marotta [8], and others [9-11]. This model distinguishes conduction through the contacting asperities and conduction through the interstitial gap. Three main modes of thermal conductance may be relevant depending on the type of deformation at the contacting asperities. The deformation can be either plastic, elastic or plastic-elastic. Typically, the deformation factor relating Young's modulus to hardness is used to distinguish the type of deformation. For plastic deformation, the heat transfer coefficient of the real contact can be calculated according to [8]:

$$h_c = 1.25 \frac{k_s m_s}{\sigma_s} \left(\frac{P}{H_c} \right)^{0.95}$$ (1)

where, k_s is the mean thermal conductivity, m_s is the mean asperity slope, σ_s is the RMS surface roughness, P is the contact pressure and H_c is the microhardness of the softer solid of the interface. For calculating the heat transfer coefficient of the interstitial gap, (2) applies in which k_g is the thermal conductivity of the interstitial medium and I_g is the gap integral which depends on the contact pressure, surface roughness and microhardness.

$$h_g = \frac{k_g}{\sigma_s} I_g$$ (2)

Microhardness is measured by making indentations that are typically 50 μm deep and therefore strongly depend on the type of surface treatment of the bulk material of the contacting solids [12, 13]. Since rack-based systems for high-end applications generally use surface treatments for

corrosion protection and wear reduction, the influence of these treatments on TCC should be considered. Equation (3) can be used to compensate for the influence of a coating on one of the contacting solids of the interface. Here, H_s is the microhardness of the softer substrate and H' is the effective microhardness of the layer substrate combination. The spreading-constriction parameter correction factor f_h accounts for heat spreading in the coated substrate. Lastly, k_1 and k_2 are the thermal conductivities of the two substrates in contact, respectively.

$$h_c{}' = h_c \left(\frac{H_s}{H'} \right) \frac{k_1 + k_2}{f_h k_1 + k_2}$$ (3)

Following (1-3), influential parameters for TCC can be translated into design parameters for a rack-based LCC system that have an impact on the thermal performance of the baseplate-cold plate interface. The first investigated design parameter is the surface roughness of the baseplate. A polished contact area with a surface roughness of Ra 0.1 μm is compared to a top-milled surface area with a surface roughness of Ra 0.3 μm. The second design parameter is the microhardness of the baseplate. The influence is analysed by comparing a conventional copper baseplate with a Vickers microhardness of 924.1 MPa to a 12 μm nickel-plated copper baseplate with a Vickers microhardness of 4.7 GPa. The last design parameter of this study is the contact pressure. Figure 4 shows the heat transfer coefficient relative to the contact pressure of four types of baseplates clamped inside an aluminium rack with an assumed surface roughness of Ra 0.6 μm. Post-processing of the baseplates is varied and include polishing, reducing the baseplate roughness from Ra 0.3 μm to Ra 0.1 μm, and nickel plating, adding a hard 12 μm layer of nickel.
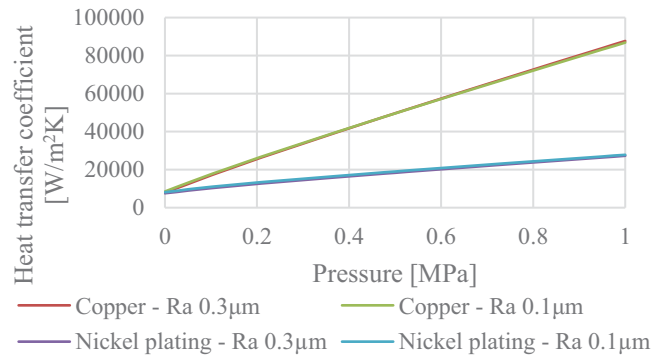

Figure 4: Modelled heat transfer coefficient of the baseplate-cold plate interface relative to the applied contact pressure.

According to the model of Yovanovich and demonstrated in the figure, the influence of the baseplate surface roughness is minute, while the option for nickel plating and the level of contact pressure both have a significant impact on the heat transfer coefficient. To test these hypotheses in practice for a rack-based LCC system, a two-level Design of Experiments is conducted with its factors and levels listed in Table 1.

Table 1: Factors and levels of the Design of Experiments.

Factor	Level 1	Level 2
Wedge-lock retainer torque	0.34 N·cm	0.68 N·cm
Baseplate surface roughness	Low (Ra 0.1 µm)	High (Ra 0.3 µm)
Baseplate surface treatment	None	Nickel 12 µm
Cold plate surface treatment	Surtec 650	Nickel 25 µm
TIM	None	Indium HSK

3   Experimental approach

The test set-up utilises a wedge-lock retainer taking the influence of its non-uniform clamping pressure on the performance of the baseplate-cold plate interface, which is difficult to predict, into account. To get an indication of the influence of the level of contact pressure on the heat transfer coefficient, the torque, by which the wedge-lock retainer is tightened, is varied between 0.34 N·cm and the specified torque by the manufacturer of 0.68 N·cm [14].

Baseplates were manufactured from copper (Cu-DHP R240) and the contact area was machined by top milling resulting in a surface roughness of Ra 0.3 µm. Afterwards, two samples were polished to a surface roughness of Ra 0.1 µm. Thereafter, two baseplates varying in roughness were electroless plated with a 12 µm layer of nickel. Finally, a separate copper baseplate was polished and tin plated with 5 µm of tin. Figure 5 shows the produced baseplates from left to right: top milled copper, nickel-plated top-milled copper, polished copper, nickel-plated polished copper and tin-plated polished copper. Note that the second baseplate has two foil heaters installed for generating a heat load. The cold plates were manufactured from aluminium (EN AW-6082 T6) and either received a Surtec 650 surface treatment or a 25 µm nickel plating.
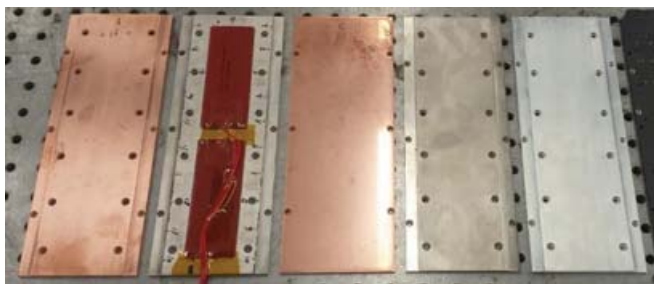

Figure 5: Copper baseplates with and without plating.

After production, the surface roughness of the baseplates and cold plates was measured using a confocal microscope (VK 9700 KEYENCE) and a stylus profiler (Mitutoyo S7-400). Figure 6 shows the roughness results for the copper and nickel-plated baseplates. The results show that electroless plating did not significantly influence the original surface roughness of the copper baseplates, which is due to uniform deposition rates of the plating process [15]. Furthermore, the Vickers microhardness of the copper and nickel-plated baseplates were measured using an indenter.
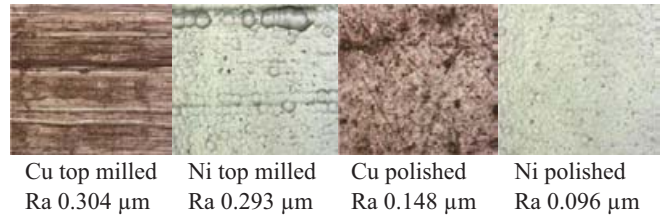

Cu top milled Ra 0.304 µm	Ni top milled Ra 0.293 µm	Cu polished Ra 0.148 µm	Ni polished Ra 0.096 µm

Figure 6: Measured surface roughness of copper and nickel-plated baseplates, top milled (Ra 0.3 µm) and polished (Ra 0.1 µm).

The experimental design also investigated the influence of a TIM. Indium HSK was selected as TIM since it is suited for burn-in applications due to the fact that its contact surface is clad with a thin diffusion barrier. This TIM can be applied in a controlled manner, it is non-toxic for humans and non-polluting for electronics, while having a relatively high TCC enhancement factor [16]. A commercial indium Heat-Spring® HSK optimized for burn-in applications [17] was also compared to plain indium cut from a sheet. It should be noted however that when joining indium to a copper baseplate, nickel plating is required as a diffusion barrier [18].

The test set-up consisted of two aluminium interface parts that provide a slot into which the baseplate was clamped. The interface parts are bolted onto a cold plate. The cold plate is liquid cooled mimicking a real LCC rack application and to reach a steady-state temperature more rapidly during testing. In order to measure the effect of the wedge-lock retainer, the temperature was measured using thermocouples along the length of the both interfaces at ten 24 mm-interval locations. Across the temperature was measured at four locations just before and after the clamped interface as shown in Figure 7. Thermocouples were placed in small holes drilled into the cold plate and baseplate. Hence, in total 40 thermocouples were used in this experimental work.
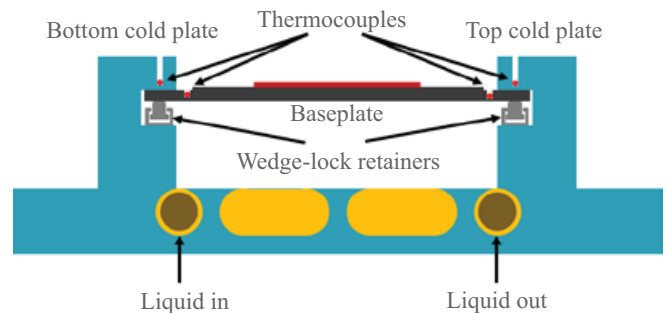

Figure 7: Schematic representation of the test set-up.

During the test procedure, a heat load was uniformly applied to the baseplate samples using two foil heaters per baseplate each dissipating 50 W. Liquid cooling came from a thermostat bath set at 10 °C with a flowrate of 6 l/min. Each test run continued until the temperature gradient across the interface remained constant. After each test run, the set-up was allowed to cool down. Before setting up a new test run, the baseplate and cold plate were cleaned using acetone. An image of the developed experimental set-up is shown in Figure 8.
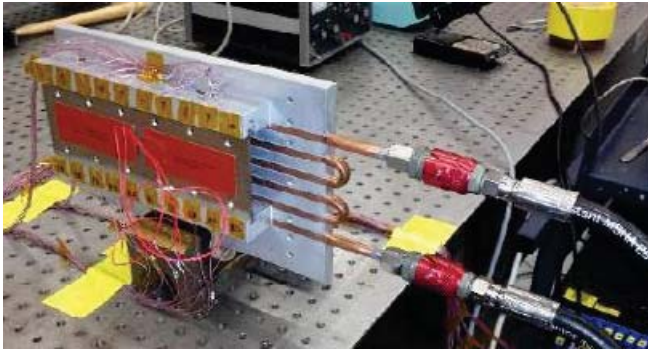
Figure 8: Image of the developed experimental set-up.

During each test run, the baseplate was fully insulated in order to gather reliable test data for the performance of the clamped interfaces. In this way, the heat load dissipated through the interface can be determined more accurately. In fact, this also replicates the thermal performance of a rack-based LRU in practice since usually multiple closely-packed modules operate at the same temperature and therefore hardly any heat transfer between modules occurs.

During each test run, temperatures were continuously recorded using a datalogger. Hence, the interface TCC was measured 20x, i.e. 10x on each slide of the baseplate. Figure 10 shows the temperature responses during the test run with the top-milled nickel-plated copper baseplate (Ra 0.3 μm) tightened at 0.68 N·cm against a Surtec 650 cold plate. As the results for the top and bottom interfaces almost perfectly align, the orientation of the baseplate and the flow direction of the liquid cooling are assumed to be insignificant. The inset in Figure 9 shows the constant temperature gradient across the interface, which is used throughout the remainder of this study. The difference between the top and bottom interfaces is only 0.7 K. Hence, for the remainder of this study both top and bottom interfaces are assumed to behave identical, effectively doubling the statistical data set.
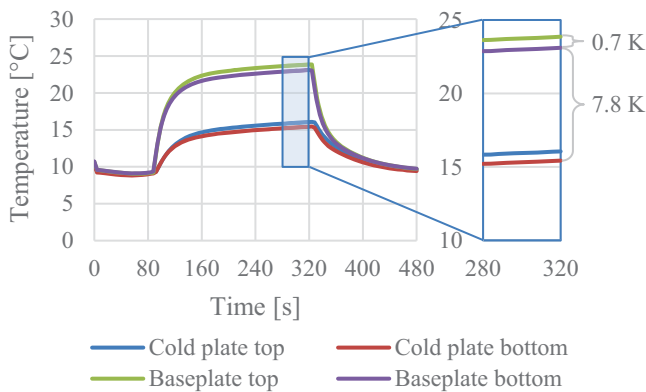

Figure 9: Temperature responses for top-milled nickel-plated baseplate (Ra 0.3 μm) clamped in a Surtec 650 cold plate.

Using the temperature responses, for each test run the interface heat transfer coefficient is computed following:

$$h = \frac{\dot{Q}}{A \cdot \overline{\Delta T}} \qquad (4)$$

where, the apparent contact area A is known from the test set-up and the temperature gradient across the baseplate-cold plate interface is represented by ΔT. For this analysis, the temperature gradient is the average constant-temperature gradient of the measured 20 interfaces and hence accounts for the non-uniformity of the clamping pressure of the wedge-lock retainer.

4 Experimental results and discussion

Figure 10 shows the experimental results for the highest contact pressure and in the case a coated aluminium rack was used. The figure illustrates the differences between copper (Cu) and nickel-plated (Ni) baseplates, between surface roughnesses of 0.3 μm and 0.1 μm, the influence of an indium TIM, and a 5 μm tin plating. The results show that focusing on the main effects of Table 1 alone is an oversimplification of the system. In accordance with Figure 4, without coating or TIM a copper baseplate performs better than a nickel-plated baseplate. For copper the influence of the surface roughness is indeed minute; however, for nickel a 27% improvement is visible, the disparity is likely due to nickel being much harder. In all cases, applying indium as TIM, being a soft and malleable metal, vastly improves the heat transfer coefficient across the interface. In comparison, heat transfer coefficients for clamped metallic interfaces reported in literature are typically around 4,000 W/m²K [19]. Hence, in some cases, using an indium TIM may already double this value. Interestingly, from a thermal perspective plain indium performs similar to the commercial version; therefore potential benefits of the commercial version should come from different perspectives, such as application, handling, storage, etc.
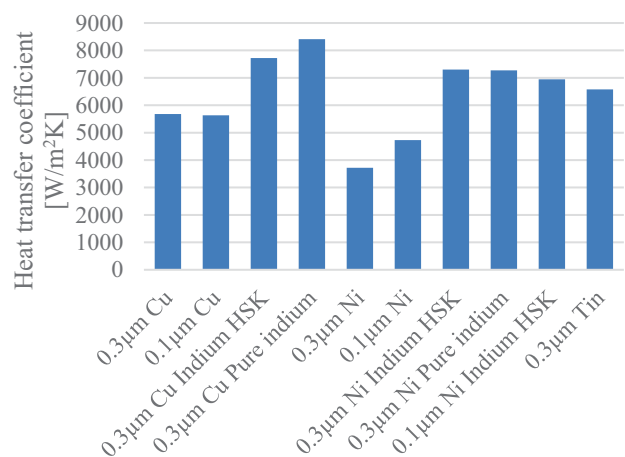

Figure 10: Experimentally determined heat transfer coefficient of copper (Cu), nickel-plated (Ni) and tin-plated baseplates, with and without a TIM. Baseplates were clamped using a wedge-lock retainer tightened at 0.68 N·cm against a Surtec 650 treated liquid-cooled aluminium rack.

Nickel plating a top-milled copper baseplate (Ra 0.3 µm) and not using a TIM reduces the heat transfer coefficient compared to the copper baseplate by 35% (from 5,680 W/m^{2}K to 3,719 W/m^{2}K). Tin plating on the other hand actually increases the heat transfer coefficient by 16% to 6,580 W/m^{2}K. This effect is likely attributed to the relatively large difference in microhardness between nickel plating (4.9GPa) and tin plating (235MPa) [20]. The tin-plated layer actually performs as a TIM in accordance with the theoretical model. In practice, a major drawback of tin plating is that cyclic mechanical loading can result in tin whiskers that in turn could lead to short circuiting [21]. Hence, although thermal very useful, tin-plating of copper baseplates will not be a viable option for electronic modules used for burn-in applications.

The heat transfer impact of the type of cold plate passivation in the case of nickel plating is significant. For the top-milled copper baseplate clamped by the wedge-lock retainer at 0.68 N·cm, the thermal performance of the interface drops by 42% from 5,680 W/m^{2}K to 3,278 W/m^{2}K when switching from a Surtec 650 treatment to a nickel-plated cold plate. The effect of the cold plate passivation on the heat transfer coefficient is not captured by the theoretical model.

The amount of torque by which the wedge-lock retainer is tightened also influences the interface performance. The heat transfer coefficient for the top-milled copper baseplate clamped into a Surtec 650 treated cold plate drops by 9% from 5,680 W/m^{2}K to 5,162 W/m^{2}K, when the torque is reduced from 0.68 N·cm to 0.34 N·cm. In theory, the contact pressure is linearly correlated to the heat transfer coefficient (see Figure 4). Due to the method of tightening using a wedge-lock retainer, which introduces friction, pretension and elasticity, this linear response could not be verified.

Lowering the surface roughness of the baseplates slightly decreased the heat transfer coefficient for the untreated copper baseplate clamped into a Surtec 650 treated cold plate. This, while lowering the surface roughness of the nickel-plated baseplate increased the interface performance by 27%. As aforementioned microhardness likely plays a role here; however, also other influencing factors that are not considered by the test set-up and theoretical model could play a role, such as e.g. surface waviness and flatness properties.

By comparing the experimental results with the modelling results, it was found that the main effects can be predicted; however, quantitatively the measured heat transfer coefficients are in all cases lower than modelled. If the wedge-lock retainer is assumed to have a uniformly distributed clamping pressure, the specified clamping force of 1,556 N with a torque of 0.68 N·cm can be translated to a clamping pressure of 1 MPa. In this case, the predicted values of the model are ten orders of magnitude higher than the experimental results. Discrepancies are likely due to perfect flatness and zero waviness assumptions, while machined surfaces are known to have these effects [22, 23]. Another parameter of the surface topology that could contribute to this discrepancy is the skewness of the asperities. In Yovanovich's model this is expressed by the effective absolute mean

asperity slope. A number of relations have been proposed to relate the asperity slope to the surface roughness; however, these correlations have reported high uncertainties [24].

To improve the model, a certain level of misalignment and non-uniform contact pressure across the interface, which is currently averaged out, should be taken into account. This is demonstrated in Figure 11, in which the temperature gradient across both interfaces due to the non-uniform contact pressure is shown. The figure shows that there indeed exists a temperature difference along the length of the baseplate-cold plate interface. The difference between both sides of the baseplate (i.e. top vs. bottom) shows that the variation is systematic and hence can be attributed to the wedge-lock retainer.
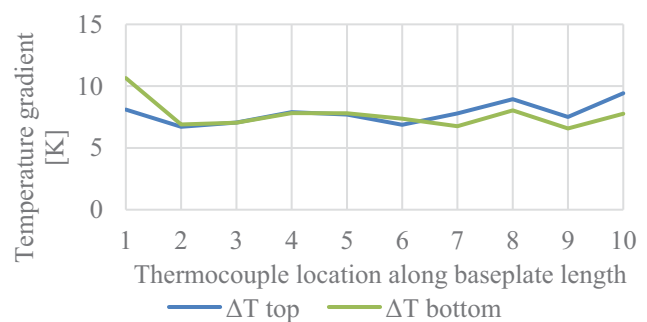

Figure 11: Temperature gradient along the length of the baseplate-cold plate interface.

To analyse the influence of each design parameter on the TCC including second-order effects, a statistical analysis of variance (ANOVA) was performed. Figure 12 shows a Pareto chart of the standardized effects in which the influence of the factors on the heat transfer coefficient is ranked by impact. As illustrated, the highest influencing factor is the passivation of the cold plate followed by the use of a TIM. Interestingly, these two factors are not present in the described theoretical model. Next with one-third of the impact is nickel plating of the baseplate. This was part of the model and in theory had the highest influence. Next in order of impact of first-order effects are torque (i.e. contact pressure) and surface roughness.
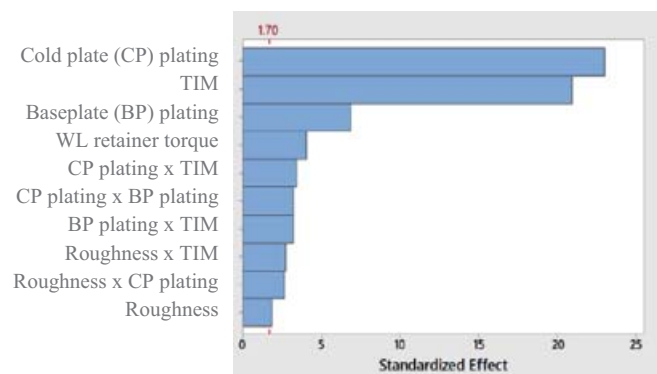

Figure 12: Pareto chart of the standardized effects with the heat transfer coefficient as response and a significance level α of 0.15.

THERMINIC 2018
((24th INTERNATIONAL WORKSHOP
on Thermal Investigations of ICs and Systems))
September 2018, Stockholm / SE
www.therminic2018.eu

Beside the first-order effects, there are a number of second-order effects that prove to have a statistical influence. In combination with a TIM, the negative influence of a nickel-plating on the baseplate or cold plate can be reduced. In this case, indium will form itself to the asperities of the nickel plating and the microhardness therefore becomes of less importance. Another second-order effect is the surface roughness in combination with a TIM. Typically without a TIM, a higher surface roughness results in lower performance. In this case however, the results are opposite, which can be explained by an increase in contact area of the interface resulting in a lower thermal resistance.

5 Conclusions

This paper presented a structured approach into analysing the thermal contact conductance between an electronics board mounted into a rack infrastructure typical for LRUs. Several design parameters that influence the interface thermal performance are analysed, such as the surface roughness, contact pressure, coating and thermal interface material. Using the developed experimental set-up and test procedure, these design parameters were analysed systematically.

The results show the limitations of theoretical models and demonstrate the importance of experimental testing of thermal contact conductance across a clamped interface. The influence of design, manufacturing and assembly parameters is quantified, which allows for an improved design of the overall cooling path; thus, extending the range of current cooling concepts. Moreover, additional design choices can be factored in, such as manufacturing and assembly cost, easy of handling during maintenance, etc. Finally, the presented test results will enhance a design engineer's awareness about thermal contact conductance.

Acknowledgements

Literature

[1] A. C. Kheirabadi and D. Groulx, "Cooling of server electronics: A design review of existing technology," *Applied Thermal Engineering,* vol. 105, pp. 622-638, 2016/07/25/ 2016.

[2] S. M. Sohel Murshed and C. A. Nieto de Castro, "A critical review of traditional and emerging techniques and fluids for electronics cooling," *Renewable and Sustainable Energy Reviews,* vol. 78, pp. 821-833, 2017/10/01/ 2017.

[3] J. Ditri, "Fluid actuated cooling card retainer," ed: Google Patents, 2014.

[4] J. C. Rozzi, T. M. Conboy, N. T. Kattamis, C. B. Munro, and J. W. Osborne, "High-Pressure Card Locks For Maximizing Heat Transfer From Electronics Cards To Card Cages," ed: Google Patents, 2017.

[5] R. D. Miller and A. D. Wachsman, "High density card retention device," ed: Google Patents, 2009.

[6] C. T. McNulty, "Sawtooth card retainer," ed: Google Patents, 1988.

[7] A. Slippey, W. G. Anderson, M. C. Ellis, C. Hose, J. Schmidt, and J. Weyant, "Thermal Management Technologies for Embedded Cooling Applications," in *2018 17th IEEE Intersociety Conference on Thermal and Thermomechanical Phenomena in Electronic Systems (ITherm)*, 2018, pp. 556-561: IEEE.

[8] M. Yovanovich and E. Marotta, "Thermal spreading and contact resistances," *Heat Transfer Handbook,* vol. 1, pp. 261-394, 2003.

[9] M. Cooper, B. Mikic, and M. Yovanovich, "Thermal contact conductance," *International Journal of heat and mass transfer,* vol. 12, no. 3, pp. 279-300, 1969.

[10] C. Tien, "A correlation for thermal contact conductance of nominally flat surfaces in vacuum," in *Proceeding of 7th Conf on Thermal Conductivity*, 1968, pp. 755-759.

[11] T. R. Thomas and S. Probert, "Correlations for thermal contact conductance in vacuo," *Journal of Heat Transfer,* vol. 94, no. 3, pp. 276-280, 1972.

[12] M. Yovanovich, "Micro and macro hardness measurements, correlations, and contact models," in *44th AIAA aerospace sciences meeting and exhibit*, 2006, p. 979.

[13] V. W. Antonetti and M. M. Yovanovich, "Using metallic coatings to enhance thermal contact conductance of electronic packages," *heat transfer engineering,* vol. 9, no. 3, pp. 85-92, 1988.

[14] Pentair, "Hoffman cooling Specifier's Guide," Pentair company guide, p. 90.

[15] R. Parkinson, "Properties and applications of electroless nickel," *Nickel Development Institute,* vol. 37, 1997.

[16] V. Sartre and M. Lallemand, "Enhancement of thermal contact conductance for electronic systems," *Applied thermal engineering,* vol. 21, no. 2, pp. 221-235, 2001.

[17] Indium Corporation, "Thermal Interface Heat-Spring® Product Guide," p. 1

[18] P. Neuhaus, C. Herzig, and W. Gust, "Grain boundary diffusion of indium in nickel and nickel-indium," *Acta Metallurgica,* vol. 37, no. 2, pp. 587-595, 1989.

[19] Jeevanashankara, C. V. Madhusudana, and M. B. Kulkarni, "Thermal contact conductances of metallic contacts at low loads," *Applied Energy,* vol. 35, no. 2, pp. 151-164, 1990/01/01/ 1990.

[20] P. Teertstra, M. Yovanovich, and J. Culham, "Calculating interface resistance," *Electronics Cooling, May issue,* 1997.

[21] W. Choi *et al.*, "Tin whiskers studied by synchrotron radiation scanning X-ray micro-diffraction," *Acta Materialia,* vol. 51, no. 20, pp. 6253-6261, 2003.

[22] C. V. Madhusudana and F. F. Ling, *Thermal contact conductance*. Springer, 1996.

[23] A. A.-H. Hegazy, "Thermal joint conductance of conforming rough surfaces: Effect of surface micro-hardness variation," 2016.

[24] A. K. Hasselström and U. E. Nilsson, "Thermal contact conductance in bolted joints," 2012.